

## Supporting Information

# Dispersive precipitation of $\text{PbI}_2$ for the optoelectronic properties preferred $\alpha\text{-FAPbI}_3$ solar cells

*Yongjun Liu*<sup>a, #</sup>, *Long Yao*<sup>a, #</sup>, *Haoyu Cai*<sup>a</sup>, *Wenjian Shen*<sup>b</sup>, *Biqi He*<sup>a</sup>, *Lingmin Liu*<sup>a</sup>,

*Wei Wang*<sup>a</sup>, *Shengqiang Xiao*<sup>a</sup>, *Juan Zhao*<sup>c, \*</sup>, *Yi-Bing Cheng*<sup>a, d</sup>, *Jie Zhong*<sup>a, d, \*</sup>

<sup>a</sup>State Key Laboratory of Advanced Technology for Materials Synthesis and  
Processing, Wuhan University of Technology, Wuhan, 430070, China

<sup>b</sup>Hubei Key Laboratory of Low Dimensional Optoelectronic Materials and Devices  
Hubei University of Arts and Science, Xiangyang 441053, P. R. China

<sup>c</sup>School of Automobile Engineering, Wuhan University of Technology, Wuhan  
430070, P. R. China

<sup>d</sup>Foshan Xianhu Laboratory of the Advanced Energy Science and Technology  
Guangdong Laboratory, Foshan 528216, Guangdong Province, P. R. China

\* Corresponding authors.

E-mail address: [juan.zhao@whut.edu.cn](mailto:juan.zhao@whut.edu.cn); [jie.zhong@whut.edu.cn](mailto:jie.zhong@whut.edu.cn)

# These authors contributed equally.

## Experimental section

Materials:

The dimethyl sulfoxide (DMSO), N,N-dimethylformamide (DMF), ethyl acetate (EA), chlorobenzene (CBZ), 4-tert-butylpyridine (tBP), lithium bis(trifluoromethylsulfonyl)imide (Li-TFSI), tris(2-(1H-pyrazol-1-yl)-4-tert-butylpyridine)-cobalt(III)tris(bis(trifluoromethylsulfonyl)imide) (FK209), and  $\text{SnCl}_2 \cdot 2\text{H}_2\text{O}$  were purchased from Sigma-Aldrich. methylammonium chloride (MACl),  $\text{C}_{60}$ , BCP, Formamidinium iodide (FAI) were purchased from Xi'an Polymer Light Technology Corp. Lead iodide ( $\text{PbI}_2$ ) and Meo-2pacz were purchased from TCI Chemicals Co. 2,2',7,7'-tetrakis (N, N-dimethoxyphenylamine)-9,9'-spirobifluorene (Spiro-OMeTAD) was purchased from Shenzhen Feiming Science and Technology Co., Ltd. Urea was purchased from Aladdin. Other materials were purchased from Sigma Aldrich Trading Co., Ltd. All materials were used as received without any further purification.

Preparation of the mixed perovskite precursor:

The mixed perovskite precursor solution was prepared by dissolving 705.35 mg  $\text{PbI}_2$ , 240.76 mg FAI, 33.76 mg MACl, in the mixture solvent of DMF/DMSO (4:1 by volume). The solution was continuously stirring for 1h before use.

Preparation of the Spiro-OMeTAD solution:

The Spiro-OMeTAD solution was prepared by dissolving 73 mg Spiro-OMeTAD into 1 mL chlorobenzene, and followed by the addition of 18  $\mu\text{L}$  Li-TFSI (pre-dissolved as a 520  $\text{mg mL}^{-1}$  stock solution in acetonitrile) and 29  $\mu\text{L}$  FK209 (pre-dissolved as a 300  $\text{mg mL}^{-1}$  stock solution in acetonitrile) and 30  $\mu\text{L}$  4-tert-butylpyridine. The solution was continuously stirring for 15 min

before use.

### **Device fabrication:**

#### 1, FTO slitting, cleaning

Firstly, tear off the packaging of 20cm \* 20cm FTO glass (Shangyang Technology), use laser to cut the FTO into small pieces of 2.5cm \* 1.25cm, and then transfer it to the glass cutting table. Cut the glass into 10cm \* 10cm blocks for cleaning. Secondly, tap water, detergent (Li Bai), and a fine bristled brush should be gently brushed on the surface of FTO and glass, and the washed glass should be placed in a customized PTFE fixture. Wash with tap water, purified water, and ethanol in sequence, and sonicate for 20 minutes. Finally, blow dry with dry air.

#### 2, CBD deposition of SnO<sub>2</sub>

First of all, the mother liquor configuration, 200 mL bottle (Shu Niu) cleaned, put a suitable size of the magnet, and injected 200 mL of pure water into the refrigerator for 2 h. Weigh 0.548 g SnCl<sub>2</sub>-2H<sub>2</sub>O, 50μL mercaptoacetic acid, 2.5 mL HCl (36% ~ 38%), 2.5 g urea to be used. The marshmallow flask, which had been cooled to contain ice water, was placed on a magnetic stirrer and stirred, and urea, hydrochloric acid, mercaptoacetic acid, and SnCl<sub>2</sub>-2H<sub>2</sub>O were added sequentially. And after stirring for 2 min, the configured masterbatch was transferred to a refrigerator for use. The FTO side of the glass needs to be UV irradiated for 15 min before CBD, and placed into the bottom of a cleaned 920 mL container (Glass Lock), in which the FTO side is placed face down. The container was filled with 100 mL of pure water and 20 mL of masterbatch, sealed using two layers of plastic wrap lengthwise and crosswise, and then covered with a lid, transferred to a 90°C oven for 3h of reaction and then removed. The FTO glass at the end of deposition was fished out and washed using pure water and blown dry using dry air. Finally, the

blow-dried FTO glass was placed on a hot bench at 180 °C for 1h, and cooled and properly placed after the end of heating.

### 3, Preparation of perovskite film

The Glass/FTO/SnO<sub>2</sub> film was cut into 2.5 cm\*1.25 cm pieces, then irradiated with UV for 15 min, and finally blown clean with dry air and transferred to the glove box for use. The above configured perovskite precursor solution was taken out using a 5 mL syringe injector (BD) and filtered through a 50 μm filter head for use. Spin-coating was performed by a two-step spin-coating method, with the first step programmed at 1000 rpm, acceleration 2000 rpm/s, and time 10 s. The second step programmed at 5000 rpm, acceleration 2000 rpm/s, and time 30 s. For spin-coating, a small piece of Glass/FTO/SnO<sub>2</sub> was taken and placed in the center of the spin-coating area of the spin-coater, and adsorbed firmly. Take 25 μL of precursor liquid and spread it on the substrate to start spin-coating; when the second step of spin-coating was carried out for 15 s, 80 μL of EA was added dropwise to the wet film; after the end of spin-coating, the film was transferred to a hot stage at 100 °C for annealing for 1 h.

### 4, Preparation of Spiro

The Spiro layer was prepared by one-step spin-coating, and the spin-coating program was set to 3000 rpm with an acceleration of 3000 rpm/s for 30 s. The Glass/FTO/SnO<sub>2</sub>/PVK film was placed in the center of the spin-coating area of the spin-coater and adsorbed firmly. Take 25 μL of precursor liquid and spread it on the substrate to start spin coating. Remove and place properly after the end.

### 5, Au electrode

The prepared Glass/FTO/SnO<sub>2</sub>/PVK/Spiro film was prepared, and the positive and negative electrodes covered by SnO<sub>2</sub>/PVK/Spiro were cleaned up under the laser, and a suitable mask plate

was fixed. Finally, the Glass/FTO/SnO<sub>2</sub>/PVK/Spiro film, which has fixed the mask plate, is fixed on the tray of the vacuum coating machine, and 80nm gold is vaporized at a speed of 0.1 nm/s.

#### 6 · Preparation of SAM, C<sub>60</sub>, BCP, Ag

The SAM layer was prepared by spin-coating method (0.5 mg Meo-2pacz was taken in advance and dissolved in 1 mL of ethanol solution, and used after shaking for 30 min), and the spin-coating program was set to 3000 rpm, with an acceleration of 3000 rpm/s for 30 s. 50 μL of the solution was taken and uniformly coated on the Glass/FTO substrate, and spin-coating was started. After the spin-coating was finished, it was placed on a hot stage at 100°C for annealing for 10 min.

C<sub>60</sub> was prepared by thermal evaporation method, and the Glass/FTO/SnO<sub>2</sub>/PVK film was fixed on the tray on the top of the evaporator to evaporate C<sub>60</sub> 25 nm at 0.1 nm/s.

BCP was prepared by thermal evaporation method, and Glass/FTO/SnO<sub>2</sub>/PVK/C<sub>60</sub> film was fixed on the tray on the top of the evaporation apparatus, and BCP 7nm was evaporated at 0.1nm/s.

Ag electrode was prepared by thermal evaporation, and Glass/FTO/SnO<sub>2</sub>/PVK/C<sub>60</sub>/BCP film was fixed on the tray on the top of the evaporation apparatus, and Ag 100 nm was evaporated at a speed of 1 nm/s.

#### **Characterizations:**

SEM images of all samples were obtained by field emission scanning electron microscopy (FESEM, JSM-7500F). All samples were characterized by X-ray diffractometer (XRD, D8 Advance) with a conventional scanning of 10 °/min. UV-vis spectrometer (Lambda 750S, PerkinElmer) was used to test the absorption spectra of samples. Mott-Schottky (M-S), SCLC and electrochemical impedance

were performed by EC-lab (SP300). The light intensity was  $100 \text{ mW}\cdot\text{cm}^{-2}$ , calibrated by a standard silicon reference solar cell (Oriel, VLSI standard). The photocurrent density-voltage curves of the perovskite solar cells were measured using a solar simulator (Oriel 94023A, 300 W) and a Keithley 2400 source meter. All devices (effective area  $0.1475 \text{ cm}^2$ ) were tested at a scanning rate of  $10 \text{ mV s}^{-1}$ . The PL and TRPL spectra were measured by a 485 nm picosecond pulsed diode laser (HORIBA Scientific Company, Japan; Nano LED-C2 N-485L). The IPCE test was characterized with an external quantum efficiency test from Newport, USA (PT-QEM1000).

## Methods

### 1. Calculation of defect state density $N_t$ by SCLC

Space charge-limited current (SCLC) is one of the common methods to test the density of defect states in semiconductor materials. Under large bias piezoelectric injection conditions, the carrier concentration in the semiconductor exceeds the equilibrium concentration, and the excess carriers form a space charge, which in turn creates a space electric field that ultimately affects the drift current. In this case, the drift current is linked to the charge concentration through Ohm's law, so that the current density, the electric field strength and the charge concentration constrain each other, and is made to be the space charge limiting current. When the applied voltage is low, the J-V curve satisfies the linear relationship; when the applied voltage is high, the J-V curve satisfies the quadratic relationship. The transition voltage of the  $J$ - $V$  curve between the linear relationship and the quadratic relationship is related to the defect concentration. Therefore, the concentration of defects can be fitted by the formula.

$$N_t = \frac{2\varepsilon_0\varepsilon V_{TFL}}{eL^2}$$

where  $\varepsilon_0$  is the vacuum dielectric constant,  $\varepsilon$  is the relative dielectric constant of the chalcogenide film (46.9),  $V_{TFL}$  is the voltage when the defect state is filled,  $e$  is the elementary charge, and  $L$  is the thickness of the perovskite film. Single-electron (FTO/SnO<sub>2</sub>/PVK/C<sub>60</sub>/BCP/Ag) and single-hole (FTO/SAM/PVK/Spiro/Au) devices were prepared to calculate the density of defect states for electrons and holes, respectively.

### 2. Calculation of built-in electric field $V_{bi}$ and defect density $N_D$ by $C$ - $V$

The capacitance-voltage characterization is an important tool for calculating the PN junction depletion region width, the built-in electric field, and the defect density. The theoretical model is to

equate the heterojunction capacitance to a parallel-plate capacitor with the depletion region as its thickness. Based on this model, the heterojunction capacitance versus bias voltage can be expressed as:

$$\frac{1}{C^2} = \frac{2(V_{bi} - V)}{e\epsilon_0\epsilon N_D A^2}$$

where  $C$  is the device capacitance,  $V_{bi}$  is the inter-device electric field,  $V$  is the external bias voltage,  $e$  is the elementary charge,  $\epsilon_0$  is the vacuum dielectric constant,  $\epsilon$  is the dielectric constant of the perovskite film,  $N_D$  is the doping density, and  $A$  is the electrode area.

### 3. Calculation of carrier lifetime by TRPL

Time-resolved photoluminescence spectroscopy (TRPL) means that under monochromatic light irradiation, photons with energy greater than the forbidden bandwidth will excite the electrons on the valence band to the conduction band; after the laser is withdrawn, the electrons on the conduction band will radiatively recombine with the holes on the valence band and emit fluorescence. By detecting the decay curve of the fluorescence intensity with time, the composite lifetime of the carriers can be fitted. This is generally fitted by a double exponential function with the following equation:

$$I(t) = I_0 + A_1 e^{-\frac{t}{\tau_1}} + A_2 e^{-\frac{t}{\tau_2}}$$

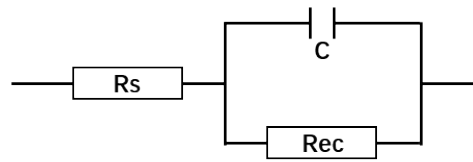
where  $I(t)$  denotes the fluorescence intensity over time, and  $\tau_1$ ,  $\tau_2$  refer to the fast decay and slow decay processes, corresponding to the composite lifetime caused by defects at the device interface

and bulk phase, respectively.  $\tau_{ave}$  can be calculated by the equation  $\tau_{ave} = \frac{A_1\tau_1^2 + A_2\tau_2^2}{A_1\tau_1 + A_2\tau_2}$ .

### 4. EIS calculation of $C$ , $R_s$ and $R_{ec}$

The equivalent circuit is shown in figure below. By fitting, we can get series resistance  $R_s$ , composite

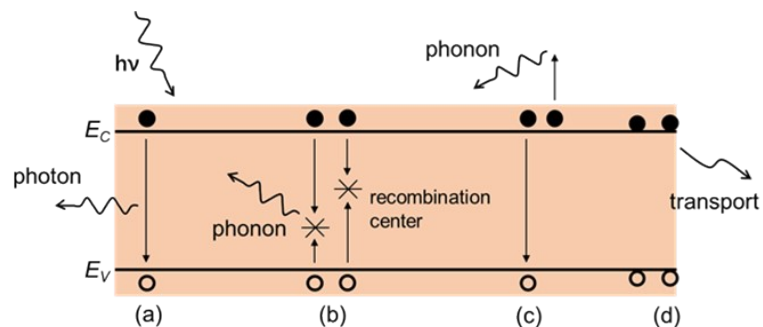
resistance  $R_{rec}$  and composite capacitance  $C$ . The product of composite resistance and composite



capacitance can reflect the carrier composite lifetime of the devices.

### 5. PL testing of photogenerated carrier generation, separation, and transport behavior on the top and bottom surfaces of films

We used 485nm laser to characterize PL. Due to the strong absorption ability of perovskite thin films towards short waves, the 485nm laser can only penetrate 80-100 nm. At this point, the photogenerated carriers cannot span the entire film without an electric field. This makes it possible to test and analyze the generation, separation, and transport behavior of photogenerated carriers at the top and bottom surfaces of Glass/FTO/SnO<sub>2</sub>/perovskite. The PL intensity of the upper surface is influenced by the generation and separation of photogenerated carriers. The PL intensity of the bottom surface is influenced by the generation and transport of photogenerated carriers.



### 6. Preparation of dry air

Firstly, high-pressure gas is prepared using an air compressor, and then dried using an adsorption dryer (Guangzhou BOLI Purification Equipment Co., Ltd). Finally, a dry gas with a dew point ranging from  $-20\text{ }^{\circ}\text{C}$  to  $-40\text{ }^{\circ}\text{C}$  is obtained.



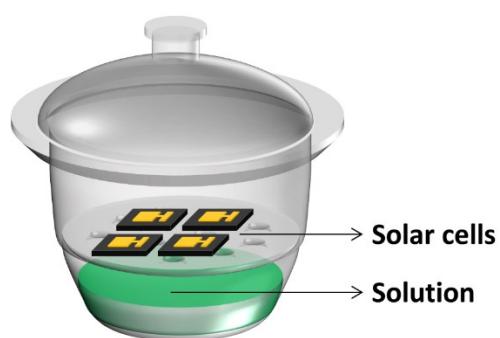


**Figure S1.** Schematic diagram of humidity control system. To explore the phase transition path of  $\alpha$ -FAPbI<sub>3</sub> under different relative humidity conditions by utilizing the law of constant relative humidity of saturated salt solution at a specific temperature.

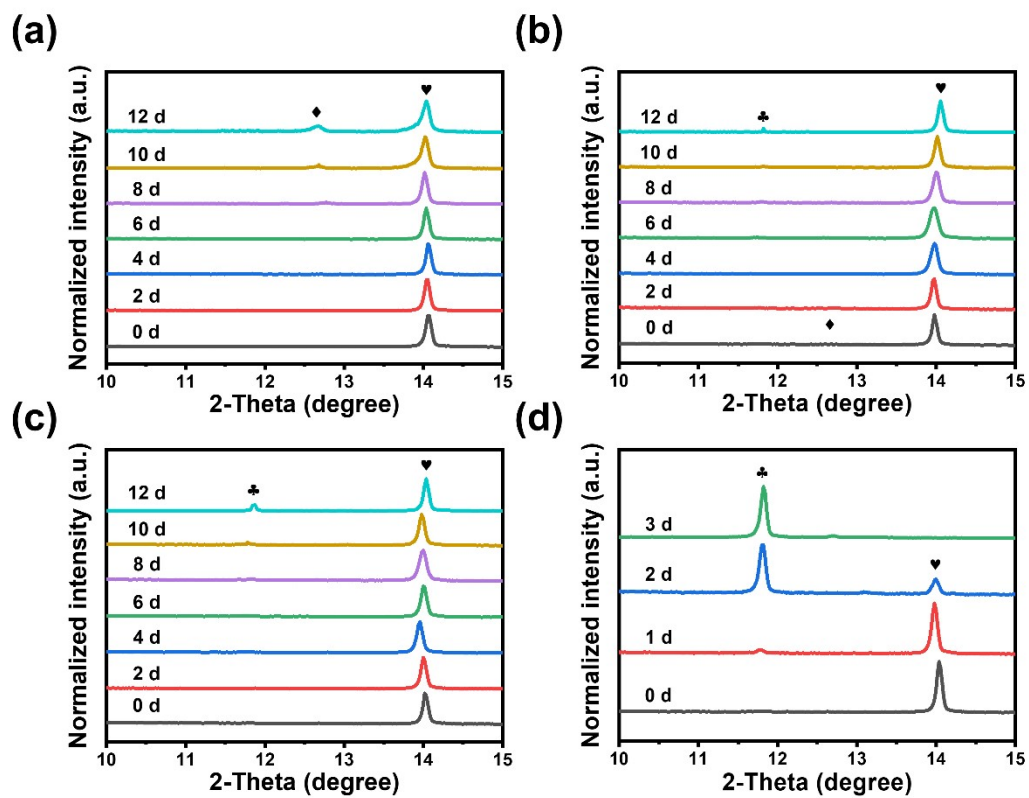


**Figure S2.** XRD of  $\alpha$ -FAPbI<sub>3</sub> phase transition path 1 (a), path 2 (b), path 3 (c) and path 4 (d). During the phase transition process, in addition to the generation of heterophase, there is also a change in  $2\theta$ .

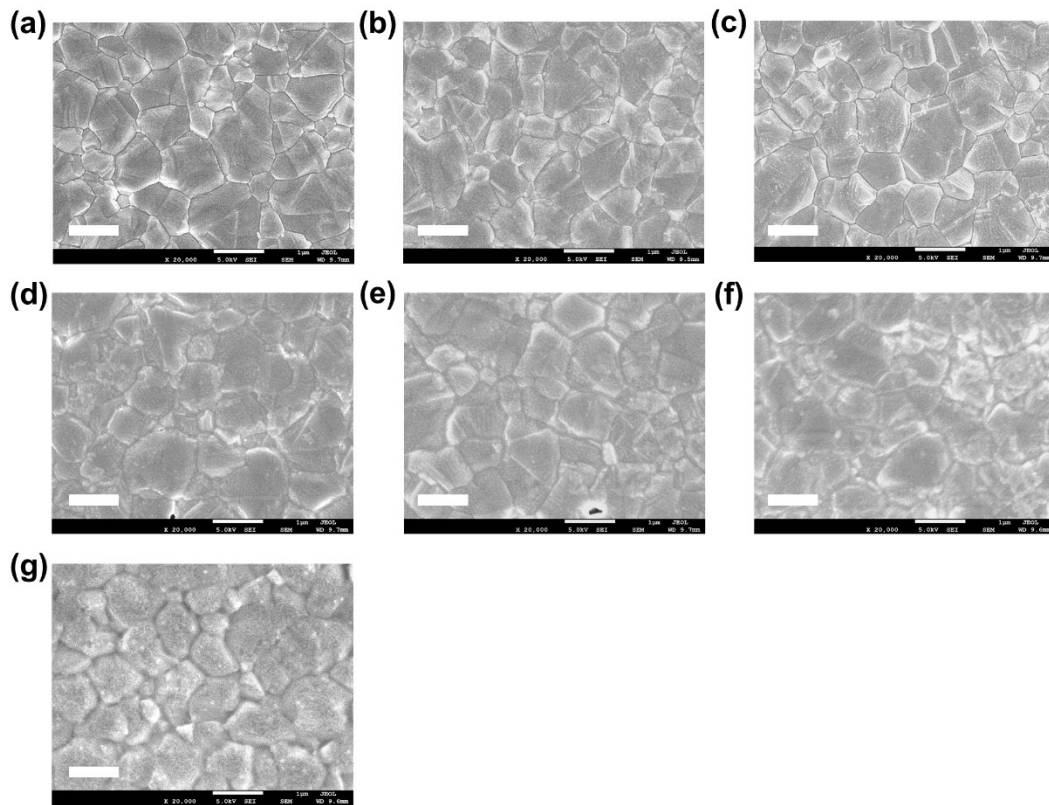


**Figure S3.** SEM of phase transition path 2. Figures a-g correspond to control, 2 d, 4 d, 6 d, 8 d, 10 d and 12 d, respectively, scale bar is 1  $\mu\text{m}$ .

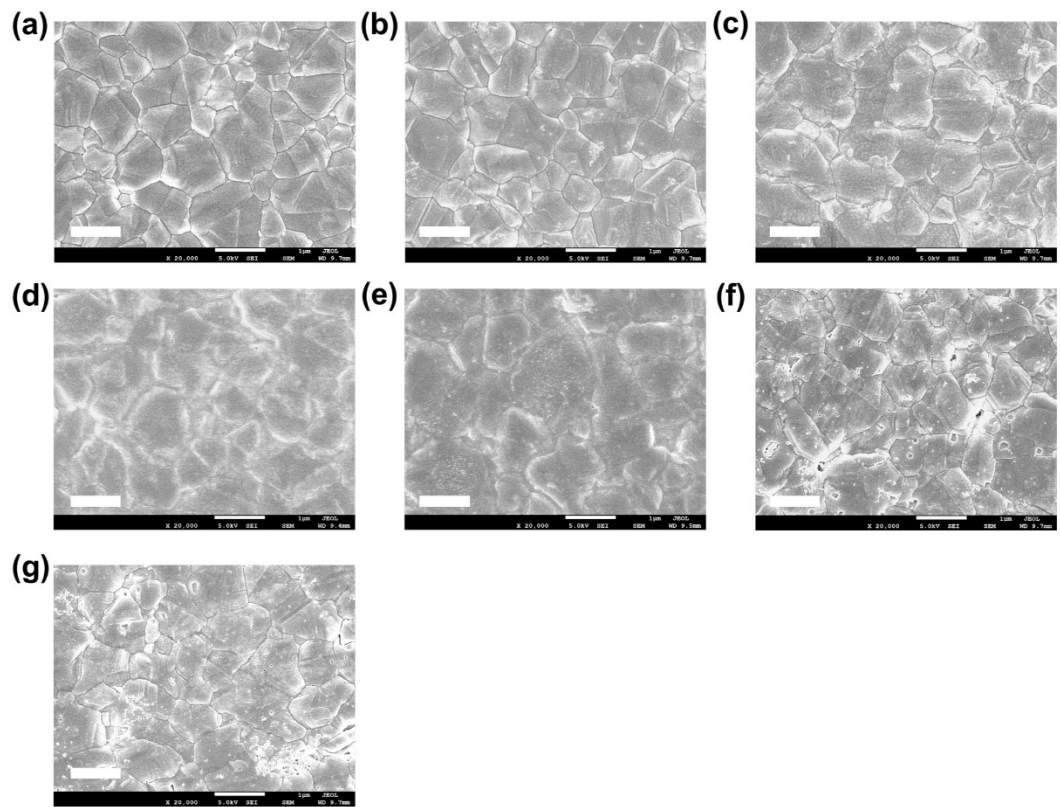


**Figure S4.** SEM of phase transition path 3. Figures a-g correspond to control, 2 d, 4 d, 6 d, 8 d, 10 d and 12 d, respectively, scale bar is 1 µm.

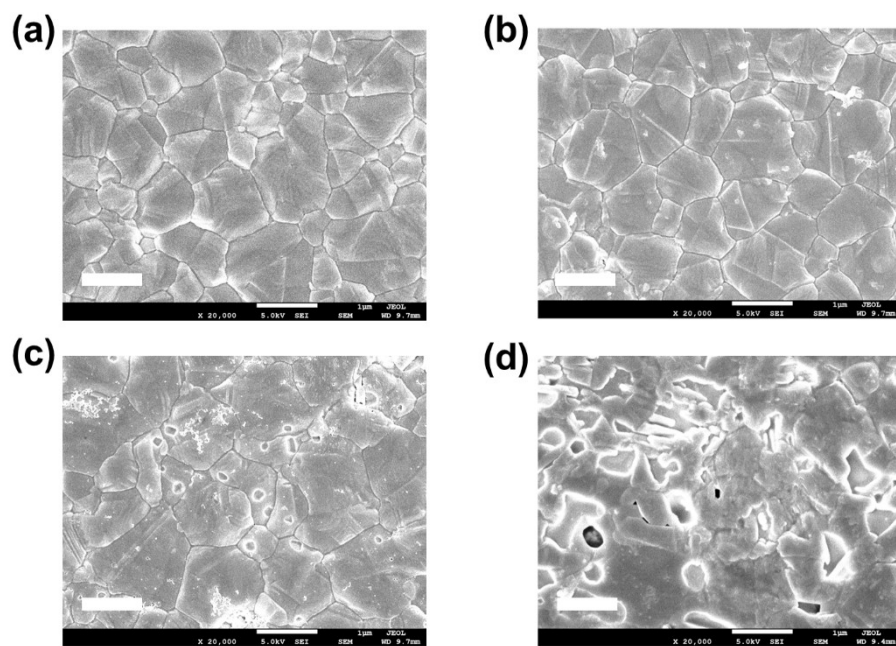


**Figure S5.** SEM of phase transition path 4. Figures a-d correspond to control, 1 d, 2 d, and 3 d respectively, scale bar is 1  $\mu\text{m}$ .

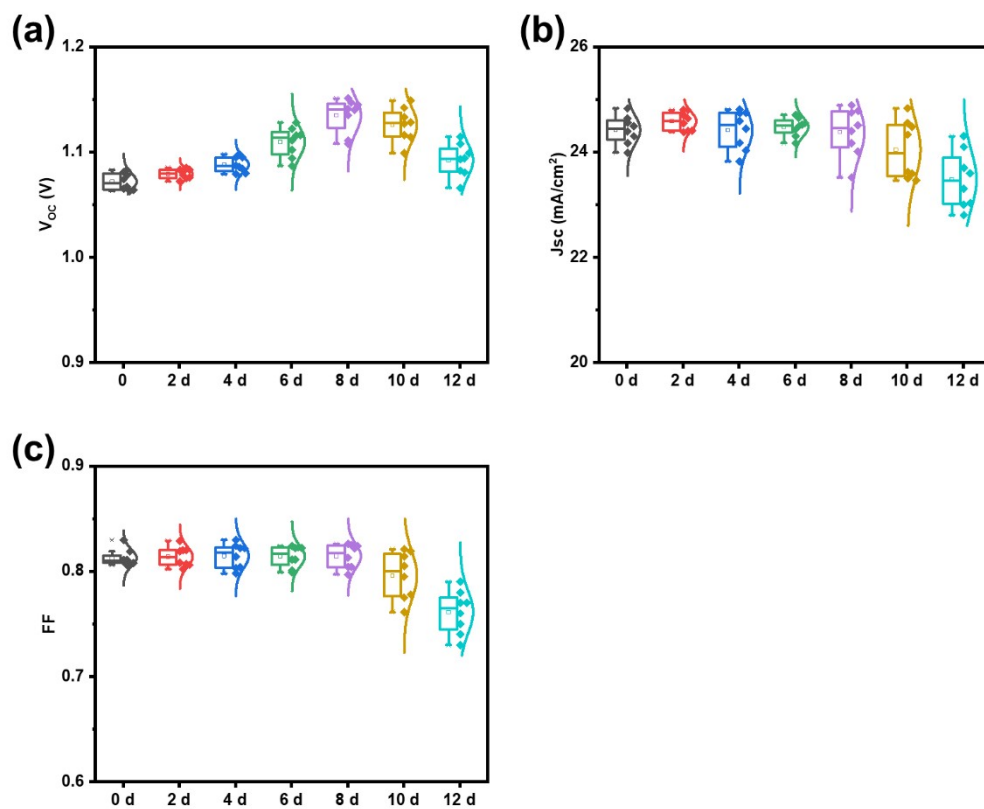


**Figure S6.**  $V_{oc}$  (a),  $J_{sc}$  (b) and FF (c) of phase transition path 1.

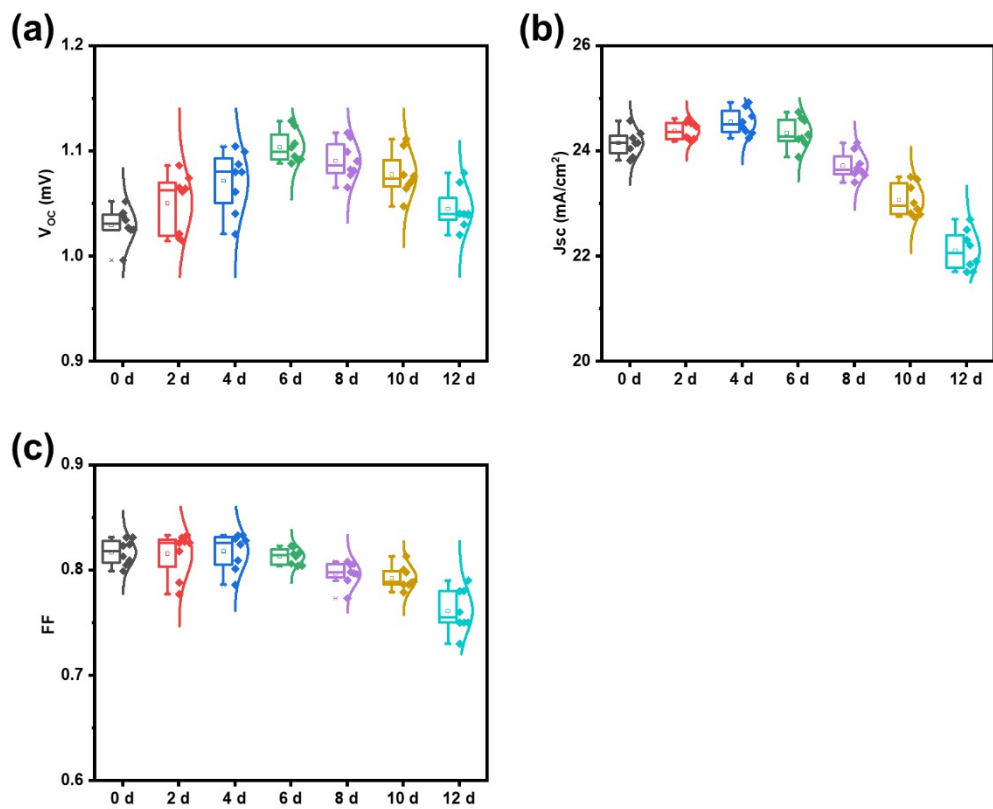


**Figure S7.**  $V_{oc}$  (a),  $J_{sc}$  (b) and FF (c) of phase transition path 2.

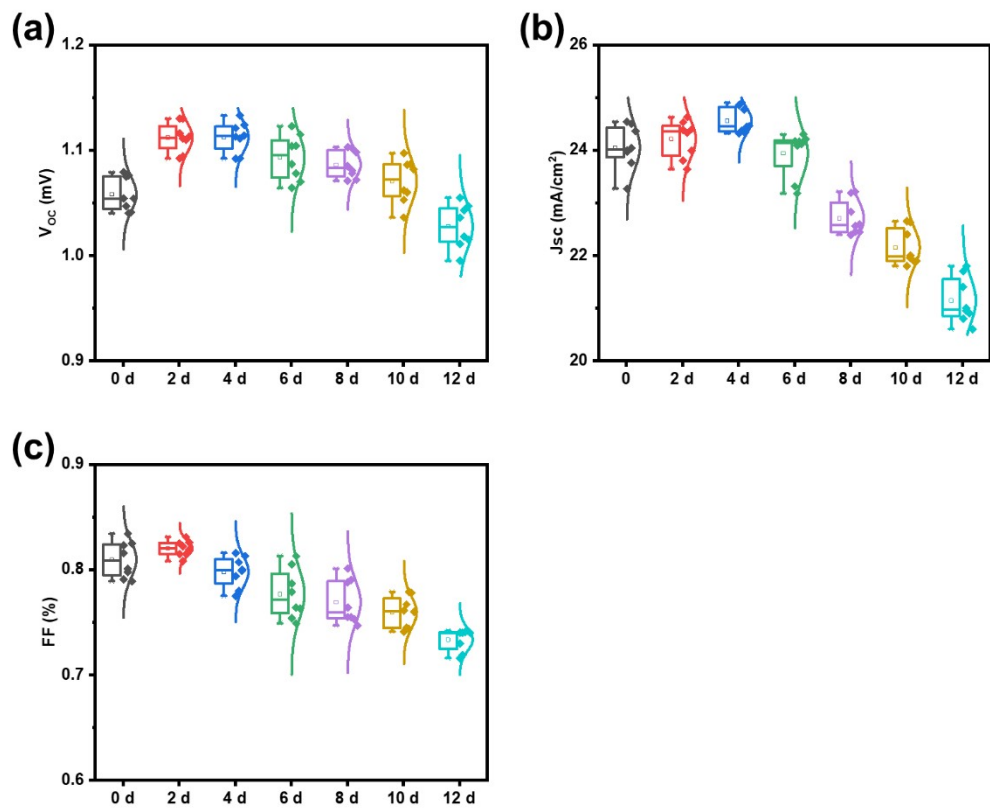


**Figure S8.**  $V_{oc}$  (a),  $J_{sc}$  (b) and FF (c) of phase transition path 3.

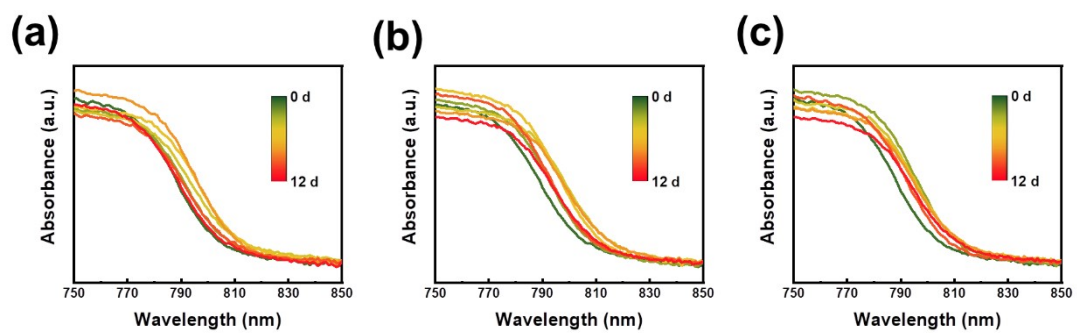


**Figure S9.** UV-Vis of phase transition path 1 (a), path 2 (b) and path 3 (c).

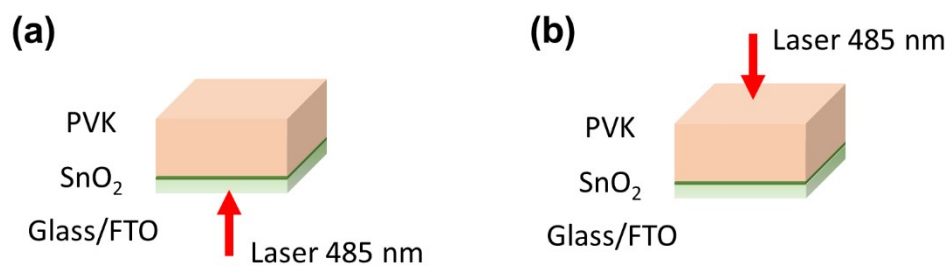


**Figure S10.** Schematic diagram of the top (a) and bottom (b) PL.

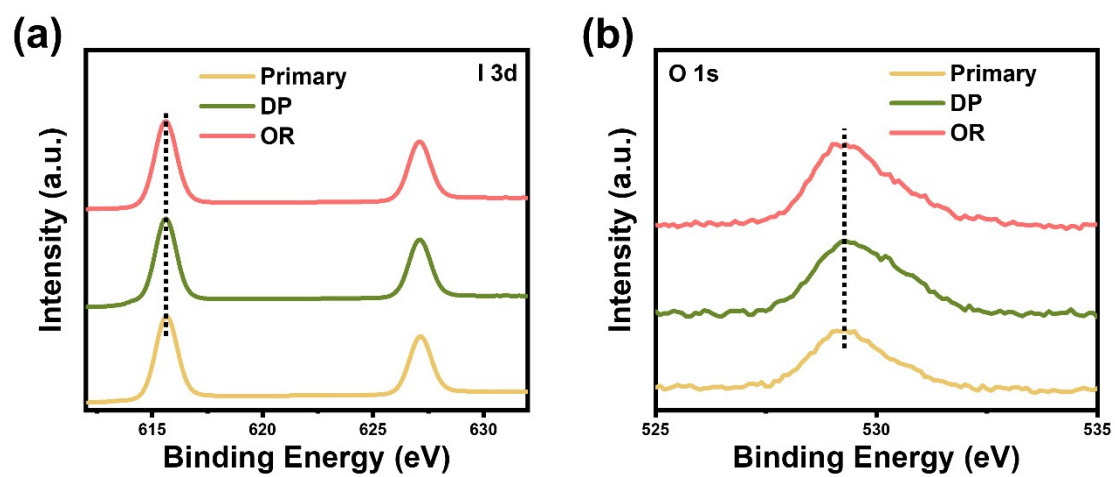
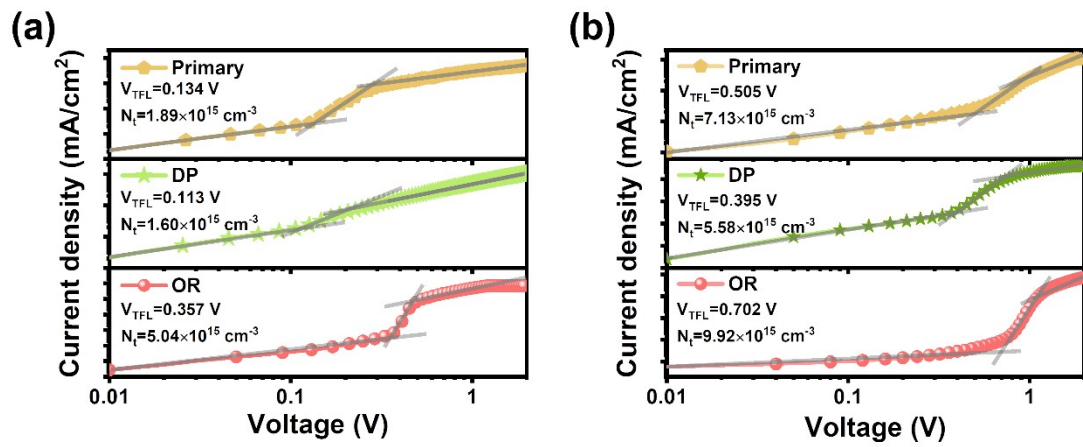


Figure S11. XPS spectra of I 3d (a) and O 1s (b) of phase transition path 1.



**Figure S12.** Dark J–V characteristics of electron-only (a) and hole-only (b) devices.

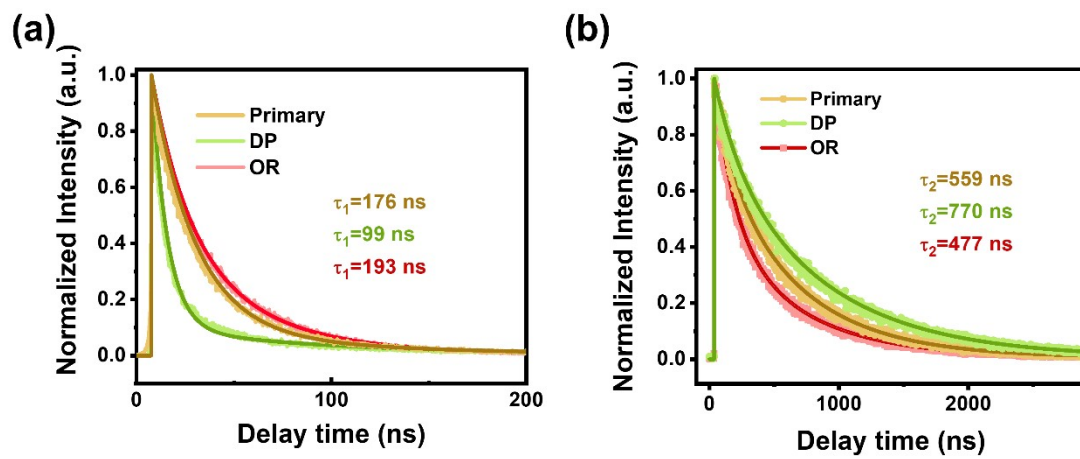
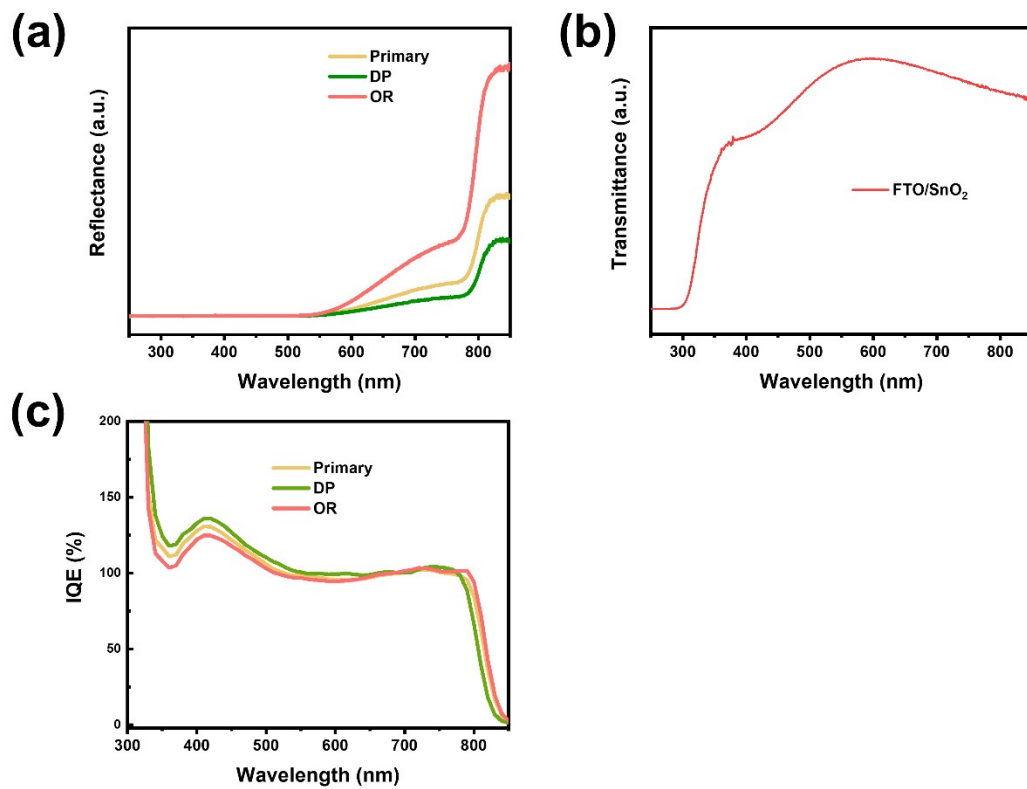


Figure S13. TRPL of Glass/FTO/SnO<sub>2</sub>/PVK (a) and TRPL of Glass/PVK (b).



**Figure S14.** Reflectance of FTO/SnO<sub>2</sub>/Perovskite/Spiro/Au (a) and the transmittance of FTO/SnO<sub>2</sub> (b). The IQE (c) of the corresponding devices was calculated using the above formula and the EQE data in the text.

**Table S1.** The dielectric constants and dipole moments of H<sub>2</sub>O (l), EA and IPA.

<b>Substance</b>	<b>Dielectric constant, <math>\epsilon</math> (20°C)</b>	<b>Dipole moment, D</b>
<b>H<sub>2</sub>O(l)</b>	81.0	2.22
<b>EA</b>	25.3	1.69
<b>IPA</b>	20.2	1.58

**Table S2.** The boiling point, saturated vapor pressure, dipole moment and geometric mean radius of NH<sub>3</sub>, HCl and H<sub>2</sub>O (g).<sup>1</sup>

<b>Substance</b>	<b>Boiling Point (°C@101kPa)</b>	<b>Saturated vapor pressure (kPa@20°C)</b>	<b>Dipole moment, D</b>	<b>Geometric average radius (Å)</b>
<b>H<sub>2</sub>O (g)</b>	100.0	2.3	1.86	1.61
<b>HCl (36~38%)</b>	61.0	14.1	1.07	1.88
<b>NH<sub>3</sub> (25~28%)</b>	37.7	48.3	1.46	1.74

**Table S3.** Equilibrium humidity of saturated solutions of different salts at 20°C.

<b>Saturated solution</b>	<b>LiCl</b>	<b>CH<sub>3</sub>COOK</b>	<b>MgCl<sub>2</sub></b>	<b>K<sub>2</sub>CO<sub>3</sub></b>
<b>RH@20°C</b>	<b>11.31±0.31%</b>	<b>23.11±0.25%</b>	<b>33.07±0.18%</b>	<b>43.16±0.33%</b>

## References

1. Dean, John Aurie, Lange's Handbook of Chemistry[M], 1978.